The Effect of ATP Analogs on Posthydrolytic and Force Development Steps in Skinned Skeletal Muscle Fibers

M. Regnier and E. Homsher
Department of Physiology, School of Medicine, University of California, Los Angeles, California 90095 USA

ABSTRACT ATP, 2-deoxy ATP (dATP), CTP, and UTP support isometric force and unloaded shortening velocity (V_u) to various extents (Regnier et al., *Biophys. J.* 74:3044–3058). V_u correlated with the rate of cross-bridge dissociation after the power stroke and the steady-state hydrolysis rate in solution, whereas force was modulated by NTP binding and cleavage. Here we studied the influence of posthydrolytic cross-bridge steps on force and fiber shortening by measuring isometric force and stiffness, the rate of tension decline (k_{Pi}) after P_i photogeneration from caged P_i, and the rate of tension redevelopment (k_{tr}) after a sudden release and restretch of fibers. The slope of the force versus [P_i] relationship was the same for ATP, dATP, and CTP, but for UTP it was threefold less. k_{tr} and k_{Pi} increased with increasing [P_i] with a similar slope for ATP, dATP, and CTP, but had an increasing magnitude of the relationship ATP < dATP < CTP. UTP reduced k_{tr} but increased k_{Pi}. The results suggest that the rate constant for the force-generating isomerization increases with the order ATP < dATP < CTP < UTP. Simulations using a six-state model suggest that increasing the force-generating rate accounts for the faster k_{Pi} in dATP, CTP, and UTP. In contrast, k_{tr} appears to be strongly affected by the rates of NTP binding and cleavage and the rate of the force-generating isomerization.

INTRODUCTION

During skeletal muscle contraction, the actomyosin interactions that generate force and shortening occur after the hydrolysis of ATP by myosin. Although much is known about actomyosin ATPase in solution, the kinetic processes in muscle fibers probably differ, owing to steric constraints imposed by the orderly array of thin and thick filaments and cross-bridge strain. When the concentration of inorganic phosphate (P_i) in contracting single skinned skeletal muscle fibers is suddenly increased by photolysis of caged P_i, the force exerted by the fiber decreases at a rate (k_{Pi}) that increases with the postphotolysis [P_i] (Millar and Homsher, 1990; Dantzig et al., 1992; Walker et al., 1992; Araujo and Walker, 1996). This behavior suggested the following kinetic scheme:

$$\begin{array}{ccc} & k_{+5} & k_{+6} \nearrow P_i \\ \ldots \leftrightarrow & AM.ADP.P_i \leftrightarrow AM^*.ADP.P_i & \leftrightarrow AM^*.ADP \rightarrow \ldots \\ & \text{no force} \quad k_{-5} \quad \text{force} & k_{-6} \quad \text{force} \end{array}$$

Scheme 1

where force is produced by an isomerization of the cross-bridge from a non-force-producing to a force-producing state and is rapidly followed and stabilized by the dissociation of P_i from the cross-bridge. Recently, measurements of k_{Pi} made during fiber shortening have suggested that the force-generating process (controlled by k_{+5}) is strain dependent, with the forward rate (k_{+5}) increasing as strain is decreased (Homsher et al., 1997).

The factors influencing the rate of force development (k_{tr}) after a sudden release and restretch of activated fibers are less well understood. k_{tr} is thought to report the rate of transition from detached or weakly attached states to a force-generating state (Brenner, 1988) and thus includes the rate(s) for strong cross-bridge attachment and force generation (Regnier et al., 1995). Therefore, if Scheme 1 is correct, k_{tr} should be similar to k_{Pi}. However, k_{Pi} is approximately twofold faster than k_{tr} in fibers under the same conditions, indicating that some process preceding the force-generating isomerization is limiting k_{tr}. This hypothesis is supported by the finding that increasing [Ca^{2+}] and [P_i] both increase k_{tr}, whereas k_{Pi} increases with increasing [P_i], but is essentially independent of [Ca^{2+}] (Millar and Homsher, 1990; Regnier et al., 1995). Furthermore, experiments using nucleotide analogs of ATP (nucleoside triphosphates or NTPs) as substrates for muscle contractions suggest that the kinetics of force development can be influenced by the rate of nucleotide binding to and cleavage by myosin, which occurs before the force-generating step (Pate et al., 1993; White et al., 1993; Regnier et al., 1998b).

To better define the actomyosin interactions that influence force development in muscle fibers, we surveyed several naturally occurring analogs of ATP (NTPs) and found that most support reduced levels of isometric force and unloaded shortening velocity in skinned muscle fibers. The reduced force and shortening velocity correlated with a lower affinity of the nucleotide for cross-bridges and/or a slower rate of NTP cleavage by acto-HMM in solution (Regnier et al., 1998a). The exception to this is 2-deoxy ATP (dATP), which supports the same level of isometric

Received for publication 28 February 1997 and in final form 16 March 1998.

Address reprint requests to Dr. Earl Homsher, Physiology Department, Center for Health Sciences, UCLA, Los Angeles, CA 90024. Tel.: 310-825-6976; Fax: 310-206-5661; E-mail: ehomsher@physiology.medsch.ucla.edu.

Dr. Regnier's present address is Center for Bioengineering, School of Medicine, University of Washington, Seattle, WA 98195-7962.

© 1998 by the Biophysical Society

0006-3495/98/06/3059/13 $2.00

force as ATP, but supports an unloaded shortening velocity that is 30% greater than that of ATP. At 10°C the dATP cleavage step by myosin is slightly slower than that of ATP, but dATP has a higher steady-state acto-HMM dATPase rate. In this paper the effects of dATP, CTP, and UTP on the rate of force production (k_{tr}) and the force-generating cross-bridge isomerization (k_{Pi}) were examined. Measurements of k_{tr} and k_{Pi} at varying [P_i] suggest that the forward rate constant of the force-generating isomerization increases in the order ATP < dATP < CTP < UTP. These measurements also suggest that the rate of force development (k_{tr}) and the [P_i] sensitivity of force development are influenced by low rates of cross-bridge detachment and nucleotide cleavage. Furthermore, k_{Pi} measurements made during fiber shortening with dATP suggest that the increased rate of force development was not due to changes in the strain dependency of the force generation cross-bridge step (k_{+5} in Scheme 1). Preliminary reports of these data have appeared in abstract form (Regnier et al., 1993; Homsher et al., 1993; Regnier and Homsher, 1996).

MATERIALS AND METHODS

Fiber preparation, solutions, and mechanical measurements

Bundles of psoas muscle fibers from female New Zealand white rabbits were used. Procedures for dissection, chemical skinning, and solution preparation were as described elsewhere (Regnier et al., 1998a; Homsher et al., 1997). The [P_i] of preactivation and activation solutions was adjusted by adding potassium phosphate at pH 7.1. All solutions contained contaminating P_i (0.7 mM; Dantzig et al., 1992) from breakdown of ATP and creatine phosphate in stock solutions, and this contamination is reflected in the [P_i] reported in the text.

All mechanical measurements were performed at 10°C. Procedures for mounting short lengths of single fibers (3–5 mm), changing solutions, and measurements of force and stiffness are described in detail elsewhere (Dantzig et al., 1992; Regnier et al., 1998a). For shortening experiments, a servo-controlled length driver (Ling 100A shaker motor) was used for variable-length quick (<2 ms) releases from isometric fiber lengths (L_o), followed by a variable isovelocity displacement. Sarcomere length was measured by laser diffraction and was set at 2.8 μm per sarcomere for all experiments, except for measurements of k_{tr}, which were made at 2.5 μm per sarcomere. Force and stiffness are designated, respectively, as P_o and S_o for ATP and as P_{NTP} and S_{NTP} for analogs of ATP, respectively. Force transients were acquired at 20 kHz and analyzed using the program KFIT (Millar and Homsher, 1990). Fibers were excluded if the control isometric force decreased by >10% during the course of the experiment. Measurements of k_{tr} were made as previously described (Brenner and Eisenberg, 1986; Brenner, 1988; Millar and Homsher, 1990). After the development of steady-state force, the fiber was allowed to shorten by applying a rapid, shortening length step of 10–15% L_o, usually for 30–40 ms. After this period of shortening, the fiber was restretched to its original length, and the rate of force redevelopment after the rapid, transient force spike was measured using a single-exponential fit. The methods for rapidly increasing the [P_i] in fibers by photolysis of caged P_i, using a frequency-doubled dye laser (UV-500; Candela, Bedford, MA), are described in detail elsewhere (Millar and Homsher, 1990; Dantzig et al., 1992). Caged P_i was synthesized and purified as described by Dantzig et al. (1992). For all photolysis experiments, preactivation and activation solutions contained 5 mM caged P_i and 10 mM dithiothreitol (DTT), and the laser was adjusted to deliver 30 mJ of UV light (measured with a Scientech 365 digital energy meter) to release ~1 mM P_i (Millar and Homsher, 1990). Contamination levels of [P_i] in the caged P_i were <2%, and this contaminating P_i, as well as caged P_i binding to cross-bridges, reduced force in activated fibers by 5–10% (Dantzig et al., 1992).

RESULTS

The NTPs selected for comparison with ATP in the present study were 2-deoxy ATP (dATP), CTP, and UTP. At a concentration of 6 mM, these NTPs support isometric force (P_{NTP}) in the order ATP = dATP > CTP > UTP and unloaded shortening velocity ($V_{u(NTP)}$) in the order dATP > ATP > CTP > UTP. The quantitative results, summarized from the accompanying paper (Regnier et al., 1998a), are shown in Table 1. The faster $V_{u(dATP)}$ correlated with a faster hydrolysis rate (NTPase), although the rates of myosin binding (K_1k_a) and cleavage of dATP ($k_{+3} + k_{-3}$) were slightly less than those for ATP. This suggests that the faster $V_{u(dATP)}$ and dATP hydrolysis rate results from differences in postcleavage rate constants. In contrast to dATP, both isometric force and V_u were reduced in CTP and UTP, with V_u being reduced to a much greater extent (Table 1). Interestingly, $V_{u(CTP)}$ did not correlate with the rate of CTP hydrolysis. The slower $V_{u(CTP)}$ and $V_{u(UTP)}$ correlate with a reduced apparent second-order binding constant (K_1k_a) for these NTPs. Measurement of the maximum $V_{u(CTP)}$ (i.e., $V_{u(CTP)}$ at saturating nucleotide) is the same as maximum $V_{u(ATP)}$, indicating that at 6 mM CTP, V_u is slowed by substrate limitation. Maximum $V_{u(UTP)}$, however, is slower than $V_{u(ATP)}$. Thus the rate of detachment of attached negatively strained cross-bridges or the rate of entry of the

TABLE 1 NTP effects on mechanical properties in muscle fibers and biochemical properties in solution

NTP	$P_{(NTP)}$	$V_{u(NTP)}$	V_u (K_m)	NTPase (s^{-1})	K_1k_a (M^{-1} s^{-1})	K_3
ATP	1.00 (129)	1.00 (78)	0.25 mM	0.92 ± 0.06	1.6×10^6	1.42
dATP	0.98 ± 0.07 (20)	1.27 ± 0.02 (20)	0.76 mM	1.01 ± 0.05	1.1×10^6	1.42
CTP	0.86 ± 2 (28)	0.52 ± 0.03 (16)	5.6 mM	0.84 ± 0.07	7.0×10^4	13.5
UTP	0.47 ± 3 (24)	0.17 ± 0.01 (10)	9.8 mM	0.31 ± 0.01	1.3×10^5	2.6

Values are from Regnier et al. (1998a) and are means ± SE (the number of observations are in parentheses). The values for force (P unloaded shortening velocity ($V_{u(NTP)}$) are normalized to values for ATP, which were 136 ± 5 kN/m^2 and 1.80 ± 0.1 ML/s, respectively. All mechanical measurements were at 200 mM ionic strength, 10°C. Mechanical data are at 6 mM NTP.

K_1k_a, Apparent second-order dissociation constant for acto-HMM in solution.

K_1, Equilibrium constant for NTP binding to acto-HMM.

K_3, Equilibrium constant for NTP cleavage by HMM (Schemes 2 and 3).

M* · UDP · P_i cross-bridge into the force-bearing states (all posthydrolysis steps) may limit shortening in UTP (Regnier et al., 1998a). Therefore, to study the postcleavage chemomechanical steps associated with force production, we measured steady-state force and the rate of force production with ATP, dATP, CTP, and UTP under a variety of conditions.

The effect of [P_i] on isometric force and fiber stiffness

The relationship between [P_i] and steady-state force is shown in Fig. 1 *a*. In each of four fibers, the effect of P_i on force was measured for all four nucleotides. The data are normalized to the maximum force produced by each NTP under control conditions (i.e., 0.7 mM P_i) to compare the relative effect of P_i on force. P_{ATP} decreased linearly with a slope of -0.43 ± 0.04 (mean ± SD) relative force units per decade increase of [P_i], in reasonable agreement with earlier work (Cooke et al., 1988; Millar and Homsher, 1990; Dantzig et al., 1992; Martyn and Gordon, 1992; Kentish, 1991). The slopes for P_{dATP} (-0.42 ± 0.03/decade [P_i]) and P_{CTP} (-0.44 ± 0.01/decade [P_i]) did not differ from ATP, suggesting that the P_i binding affinity of cross-bridges was not affected by NTPs. In contrast to ATP, dATP, and CTP, the P_i sensitivity of P_{UTP} was small (Fig. 1 *a*) but significant (-0.14 ± 0.01/decade [P_i]), and S_{UTP} was not affected by increasing [P_i] (at least up to 10.7 mM P_i). To determine if the reduced affinity of UTP for myosin causes the reduced P_i sensitivity of force in NTP, we measured the isometric force and stiffness at a low concentration of ATP (0.25 mM). Reduction of [ATP] increased isometric force by ~15%, but had no effect on the slope of P_{ATP} (-0.42 ± 0.01/decade [P_i]; data not shown), suggesting that lower substrate availability does not affect the P_i sensitivity of isometric force. These results further suggest that, when UTP is the substrate for isometric contractions, a smaller fraction of cross-bridges are in a state that can bind P_i. A similar lack of P_i sensitivity of force has been reported for GTP (Pate et al., 1993).

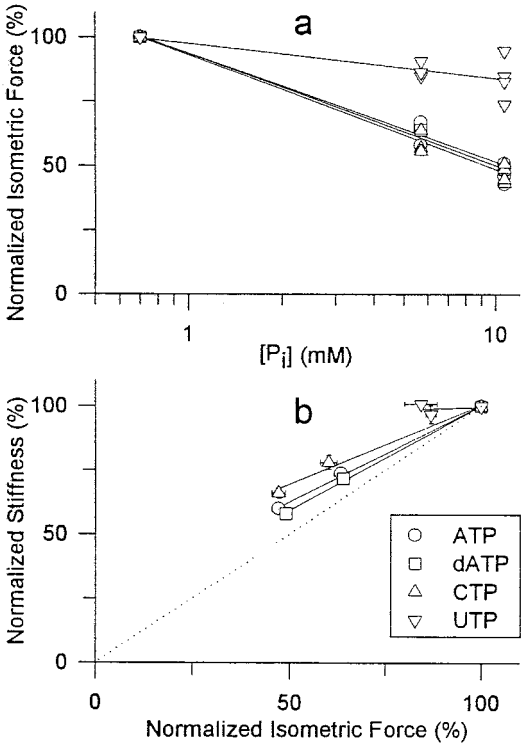

FIGURE 1 Effects of [P_i] on force and the force-stiffness relationship in muscle fibers. (*a*) Steady-state isometric force was compared for ATP, dATP, CTP, and UTP in each of four fibers in the presence of 0.7, 5.7, and 10.7 mM P_i. Force was reduced linearly with log [P_i] for all of the NTPs. (*b*) Stiffness-force relationship for NTPs at the same P_i concentrations as in *a*. Here the mean ± SE of the same four fibers as in *a* are displayed. Some SE values are smaller than the symbol size. Stiffness at 10 mM P_i was greater for CTP than for ATP or dATP ($p < 0.05$), and stiffness was not significantly reduced for UTP at either 5.7 or 10.7 mM P_i. Force and stiffness were remeasured for ATP (0.7 mM P_i) at the conclusion of the experiments and were unchanged from their original values. The slopes of the force-[P_i] and stiffness-[P_i] relationships are given in the text.

Fiber stiffness with no added P_i was the same with ATP (1.0), dATP (0.99 ± 0.06 SE, $n = 8$), and CTP (1.02 ± 0.06 SE, $n = 6$), but was significantly reduced in UTP (0.65 ± 0.05 SE, $n = 10$). The stiffness relative to isometric force increased with CTP and UTP however, suggesting either 1) that a population of cross-bridges that contributes to stiffness but not to force is increased; or 2) that the average force per cross-bridge is decreased for these two nucleotides. Fiber stiffness (S_{NTP}) also declined linearly with log [P_i] in ATP, dATP, and CTP, but the slopes for S_{ATP} (-0.33 ± 0.04/decade [P_i]), S_{dATP} (-0.34 ± 0.03/decade [P_i]), and S_{CTP} (-0.27 ± 0.04/decade [P_i]) were less steep than the slopes of P_{NTP} versus [P_i] (not shown). This is best seen by plotting P_{NTP} versus S_{NTP} with increasing [P_i] (Fig. 1 *b*). The relatively greater effect of [P_i] on P_{NTP} (compared to S_{NTP}) suggests that elevating [P_i] increases a population of non-force-bearing cross-bridges that contribute to fiber stiffness, but either do not exert force or exert less force than AM · ADP (Regnier et al., 1995).

Measurements of force redevelopment (k_{tr}) in fibers

To characterize how different NTPs alter the kinetics of force generation, we measured the rate of force redevelopment (k_{tr}) after a brief period of unloaded shortening (Brenner and Eisenberg, 1986). Sample k_{tr} traces for ATP, dATP, CTP, and UTP (in the same fiber) are shown in Fig. 2, *a* and *b*. The force transient after restretching of the fiber is similar for ATP and dATP (Fig. 2 *a*), with a rapid force spike that also decays rapidly, followed by a slower rise in force that is well fitted by a single exponential rate constant. For these traces, k_{tr} was ~25% faster in dATP (14 s^{-1}) than that in ATP (11 s^{-1}), a finding that was consistent for all measurements (Table 2). In Fig. 2 *b* the trace for ATP is redrawn to compare with k_{tr} traces for CTP and UTP. When CTP or UTP are the substrates for contraction, the rapid force spike

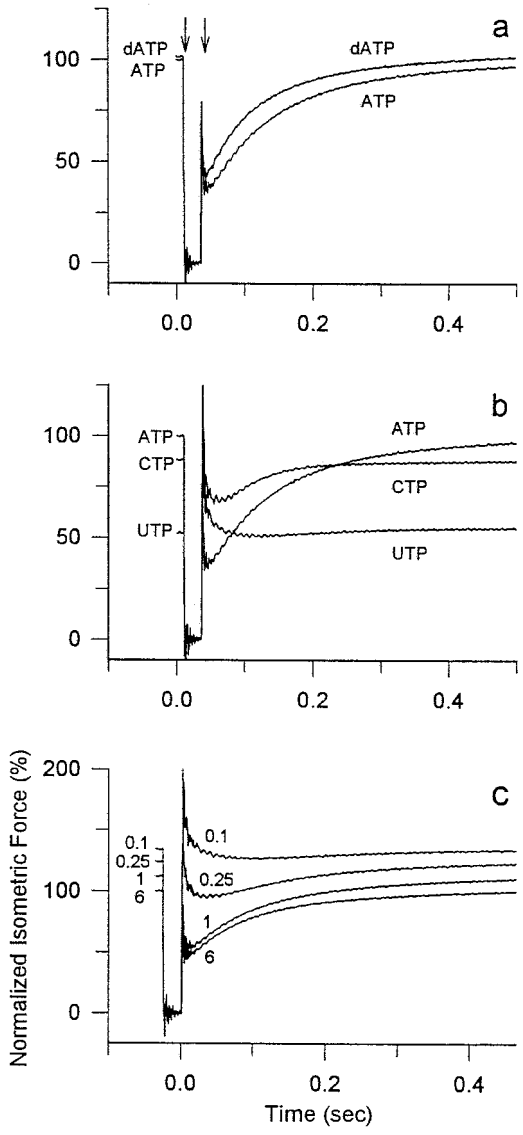

FIGURE 2 Sample k_{tr} records. Comparison of ATP versus dATP (*a*) and ATP versus CTP and UTP (*b*) in the same fiber. Force values are normalized to maximum isometric force for 6 mM ATP (154 kN/m^2, CSA = 3846 μm^2). k_{tr} for this fiber is 11 s^{-1} (ATP), 14 s^{-1} (dATP), 17 s^{-1} (CTP), and 5 s^{-1} (UTP). The starting force after the restretch of the fiber (A_{tr}; % steady-state force) is 35% (ATP), 43% (dATP), 65% (CTP), and 92% (UTP). (*c*) Effects of varying [ATP] on k_{tr}. This fiber is different from the one in *a* and *b*, and at 6 mM ATP force was 141 kN/m^2 (CSA = 3897 μm^2). The relative force, k_{tr}, and A_{tr} for this fiber were 1.34, 5 s^{-1}, and 95% (0.1 mM ATP); 1.24, 5 s^{-1}, and 76% (0.25 mM ATP); 1.12, 11 s^{-1}, and 53% (1 mM ATP); and 1.0, 12 s^{-1}, and 44% (6 mM ATP).

from restretching the fiber is larger and decays much more slowly than for ATP or dATP. The result is that the slow rise of force becomes apparent at a much greater force level. However, this slow rise is still fit well by a single exponential, similar to ATP and dATP. The measurable k_{tr} was faster for CTP (17 s^{-1}) and slower for UTP (5 s^{-1}) than for ATP. Because CTP and UTP have a lower affinity for myosin than ATP, we reduced the concentration of ATP to determine if differences in k_{tr} resulted from lower substrate availability (Fig. 2 *c*). Reducing the concentration of ATP did result in records similar in shape to those of CTP and UTP and reduced k_{tr}. Reduced substrate availability does not completely explain the changes in k_{tr} with CTP and UTP, however, because reducing [ATP] increases steady-state force (as opposed to a 50% reduction with UTP), and k_{tr} with CTP is faster, not slower.

TABLE 2 Force transients resulting from release of P_i from caged P_i photolysis and release-restretch cycles

NTP	A_{P_i} (% P_{NTP})	k_{P_i} (s^{-1})	k_{tr} (s^{-1})
ATP	18 ± 0.8	23 ± 1 (45)	11 ± 1 (45)
dATP	19 ± 1.2	28 ± 1 (28)	14 ± 1 (13)
CTP	14 ± 0.7	42 ± 2 (9)	16 ± 2 (11)
UTP	9.0 ± 0.8	61 ± 7 (6)	5 ± 1 (10)
0.25 mM ATP	15 ± 1.0	15 ± 1 (5)	5 ± 2 (7)

All values were significantly different from 6 mM ATP ($p < 0.01$), except A_{P_i} for dATP.
Figures in parentheses are the number of observations.

When ATP is the substrate for contraction, k_{tr} increases with increasing [P_i], even though steady-state force decreases (Metzger and Moss, 1991b; Regnier et al., 1995). Sample k_{tr} traces, at three P_i concentrations, are shown in Fig. 3 *a*. Fig. 3 *b* are recordings from Fig. 3 *a* normalized to steady-state force levels before the release-restretch cycle. These records show that increasing [P_i] affects force transients in a manner comparable to that of CTP: i.e., steady-state force is reduced while k_{tr} is increased. On the other hand, force transients with UTP appear to combine the properties of decreased steady-state force seen with high [P_i] and the reduction in k_{tr} seen with low substrate availability. Increasing the [P_i] of activation solutions also increases k_{tr} (Fig. 4 *a*) and the starting amplitude of the slow rise in force (A_{tr}; Fig. 4 *b*) with dATP, CTP, and low ATP (0.25 mM). The results for CTP are in agreement with those Wahr et al. (1997). k_{tr} increases according to the series UTP ≤ low ATP < ATP < dATP < CTP over the range of P_i concentrations used for these studies. The similar slopes of the k_{tr} versus [P_i] plots for ATP, dATP, and CTP suggest that the P_i binding affinity of cross-bridges is similar for these nucleotides, in agreement with the steady-state force data (Fig. 1), and that the mechanism by which P_i regulates k_{tr} is not greatly altered by these NTPs.

Measurements of the isometric phosphate transient (k_{Pi})

An estimate of the rate constant for the force-generating isomerization was obtained by measuring the rate of force decline after the photorelease of P_i from caged P_i. Sample recordings of these P_i-induced force transients (P_i transients) are shown in Fig. 5. Records on the left side of the figure show the steady-state force levels for dATP (*a*), CTP (*c*) and UTP (*e*), before photolysis of caged P_i, and changes in tension resulting from a rapid 1 mM increase in [P_i] (from

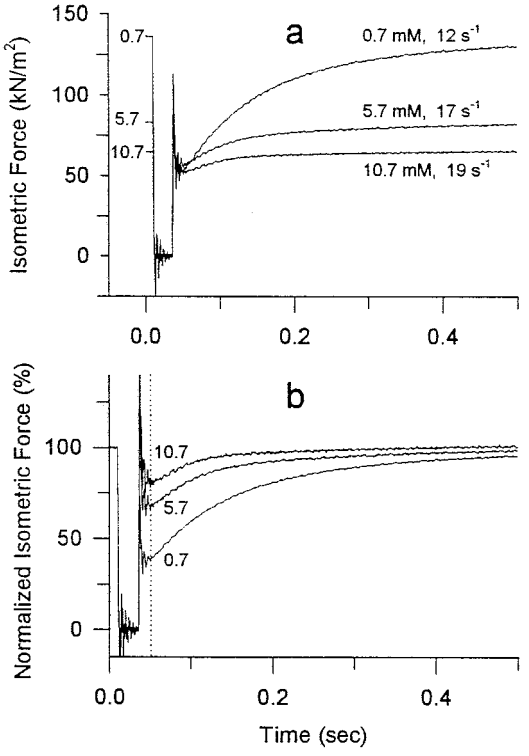

FIGURE 3 Sample k_{tr} recordings at three different P_i concentrations in the same fiber. Records in *a* show the steady-state force produced before a rapid, 10% length step and the force development characteristics upon restretching of the fiber to its original length. The $[P_i]$ and single exponential fit rate (in s^{-1}) are indicated for each trace in the figure. In *b* recordings from *a* were normalized to the steady-state force measured just before fiber release to show that the relative starting amplitude (A_{tr}) increases as the $[P_i]$ is increased. The vertical dotted line indicates the beginning of the data fitting routine.

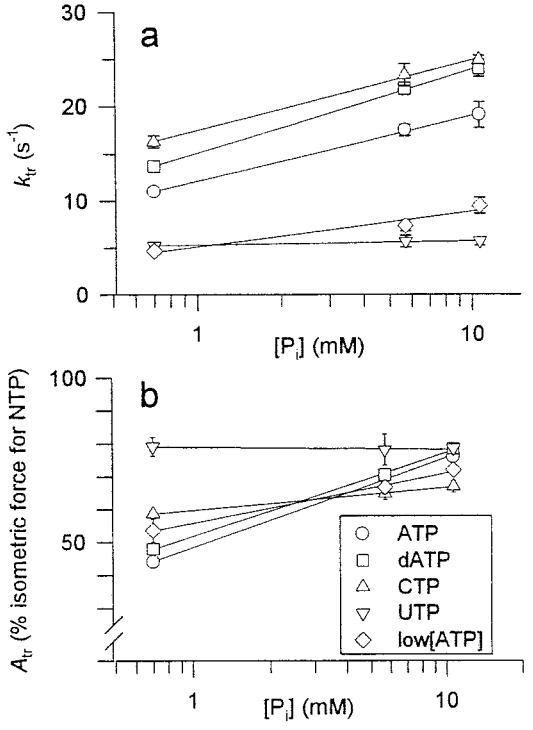

FIGURE 4 Summary of effects of $[P_i]$ on k_{tr} (*a*) and the force level at the beginning of the measurable transient A_{tr} (*b*) with ATP (0.25 mM and 6 mM), dATP (6 mM), CTP (6 mM), and UTP (6 mM). The number of comparative observations ranged from 10 to 13 for each NTP, except 0.25 mM ATP, where $n = 5$. Lines are linear fits to the data with slopes of (in s^{-1}/decade $[P_i]$) (*a*) 7.0 (ATP), 8.7 (dATP), 8.7 (CTP), 0.4 (UTP) and 3.7 (0.25 mM ATP); and (in percentage of NTP isometric force/decade $[P_i]$) (*b*) 27.4 (ATP), 25.6 (dATP), 7.0 (CTP), 0.0 (UTP), and 15.3 (0.25 mM ATP).

0.7 mM to 1.7 mM). P_i transients with ATP (in the same fiber) are shown for comparison. On the right side of the figure (Fig. 5, *b*, *d* and *f*, respectively), records from the left side were normalized to their preflash force to compare the relative effects of increased P_i on the rate (k_{Pi}) and the amplitude (A_{Pi}) of the force decline. Measurements of A_{Pi} were influenced by a slow rising phase that occasionally followed the initial rapid relaxation of force with ATP (see ATP trace in Fig. 5 *c*). This slow rise in force was more consistently seen in dATP, and always occurred in CTP and UTP. The force rebound was small relative to the P_i transient amplitude ($\leq$10%) for ATP or dATP, but was much larger, with a relatively steep slope, for CTP and UTP (see Discussion). To account for this, a single exponential fit with a rising slope was used to measure k_{Pi} and A_{pi} from the traces normalized to preflash steady-state force (i.e., Fig. 5, *b*, *d* and *e*). k_{Pi} for these traces increased in the order ATP $<$ dATP $<$ CTP $<$ UTP, whereas A_{Pi} decreased in the order ATP = dATP $>$ CTP $>$ UTP (see Fig. 5). This order was consistent for all experimental observations; the data are summarized in Table 2. dATP increased k_{Pi} by ~20% and had no significant effect on A_{pi}. CTP and UTP increased k_{Pi} by two- to threefold, but decreased A_{Pi}. Reducing the [ATP] from 6 mM to 0.25 mM (Fig. 5, *g* and *h*) produced a small reduction in A_{Pi} (15%), but resulted in a slower (35%), not faster, k_{Pi} (summarized in Table 2). Increasing [CTP] or [UTP] from 6 to 10 mM had no effect on k_{Pi} (data not shown). These results suggest that the faster, smaller P_i transients with CTP and UTP did not result from slower substrate binding to cross-bridges.

At low concentrations of $[P_i]$, k_{Pi} increased in a linear manner with $[P_i]$ when ATP was the substrate for contractions. The *y*-intercept of this relationship is an estimate of the forward rate constant of the force-generating step (k_{+5} in Scheme 1) (Dantzig et al., 1992; Walker et al., 1992). k_{Pi} also increased as the $[P_i]$ was increased in dATP and CTP. Sample P_i transients with dATP at three different starting P_i concentrations (in the same fiber) are shown in Fig. 6 *a*. As $[P_i]$ increased, steady-state force decreased, and photorelease of an additional 1 mM P_i resulted in a faster k_{Pi} and a smaller A_{Pi} (as predicted from Fig. 1 *a*). This behavior is better seen in Fig. 6 *b*, in which the traces from Fig. 6 *a* are replotted and normalized to prephotolysis steady-state force for measurement of k_{Pi} and A_{Pi}. The effects of $[P_i]$ on k_{Pi} and A_{Pi} are summarized in Fig. 7, *a* and *b*, respectively. Linear regression of the data yielded *y*-intercepts of 15 s^{-1} for ATP, 19 s^{-1} for dATP, and 35 s^{-1} for CTP, with similar

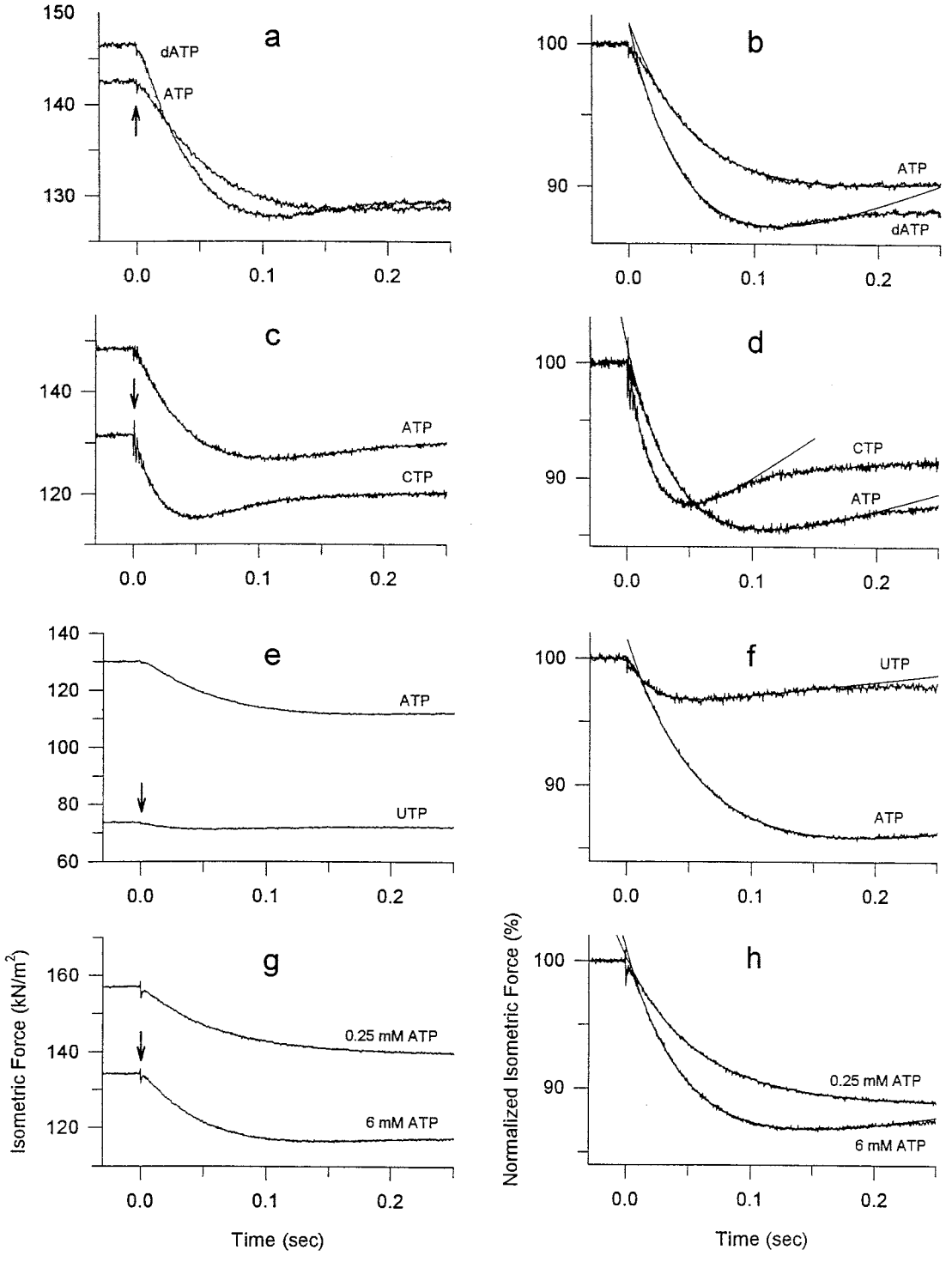

FIGURE 5 Sample P_i transients with varying NTP. Traces on the left side of the figure show the absolute magnitude of isometric force and the P_i transients for comparison of ATP with dATP (*a*), CTP (*c*), and UTP (*e*). The corresponding traces on the right show the same traces normalized to preflash isometric force (*b*, *d*, and *e*, respectively). (*g* and *h*) Absolute and normalized traces comparing ATP (6 mM) versus low ATP (0.25 mM), respectively. All of the transients were fit well with a single exponential fit (*lines* in *b*, *d*, *f*, and *h*). k_{Pi} and A_{Pi}, measured from the normalized traces, are as follows: (*b*) k_{Pi}, 21 s^{-1} (ATP), 26 s^{-1} (dATP); A_{Pi}, 11% (ATP), 16% (dATP): (*d*) k_{Pi}, 27 s^{-1} (ATP), 58 s^{-1} (CTP); A_{Pi}, 19% (ATP), 16% (CTP): (*f*) k_{Pi}, 20 s^{-1} (ATP), 63 s^{-1} (UTP); A_{Pi}, 18% (ATP), 7% (UTP): (h) k_{Pi}, 23 s^{-1} (6 mM ATP), 17 s^{-1} (0.25 mM ATP); A_{Pi}, 17% (6 mM ATP), 11% (0.25 mM ATP).

slopes for all three nucleotides (see Fig. 7), suggesting that k_{+5} increases in the order ATP < dATP < CTP. P_i transients with UTP were measured only at a low [P_i] because the small amplitude of the transients made k_{Pi} and A_{Pi} difficult to measure. However, k_{Pi} for a 1 mM increase in [P_i] (from 0.7 mM to 1.7 mM P_i) was greater for UTP (61 ±

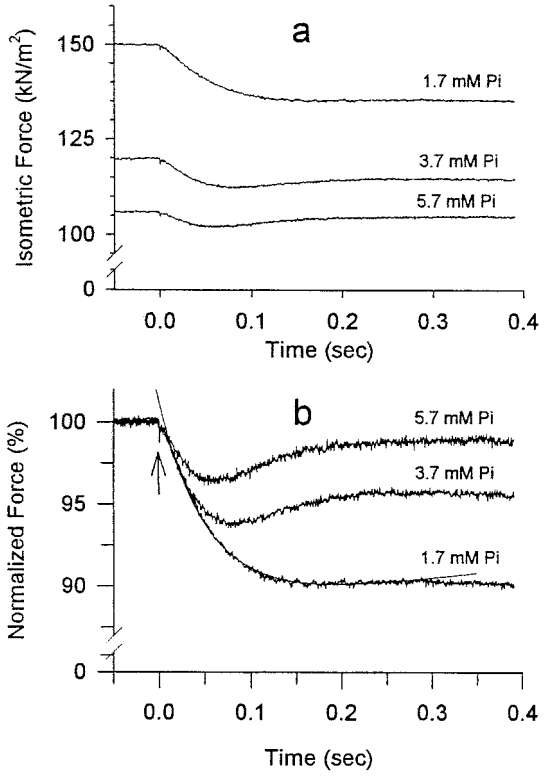

FIGURE 6 Sample traces showing the effects of increasing $[P_i]$ on the P_i transient using dATP (in the same fiber). Fibers were fully activated to steady-state isometric force, then 1 mM P_i was photogenerated, resulting in force relaxation transients. In *a* the starting force level is designated for each $[P_i]$, and the final $[P_i]$ is designated near the end of the trace. Increasing the starting $[P_i]$ resulted in less preflash isometric force and smaller, faster P_i transients. In *b* k_{Pi} and A_{Pi} were measured from traces normalized to preflash isometric force. k_{Pi} values for these records were 20 s^{-1}, 27 s^{-1}, and 34 s^{-1} for 1.7 mM, 3.7 mM, and 5.7 mM final $[P_i]$, respectively, and the corresponding A_{Pi} values were 14%, 11%, and 7%. A flash (indicated by the *arrow*) artifact and the single-exponential fit for the 1.7 mM P_i trace (*solid line*) are shown in *b*.

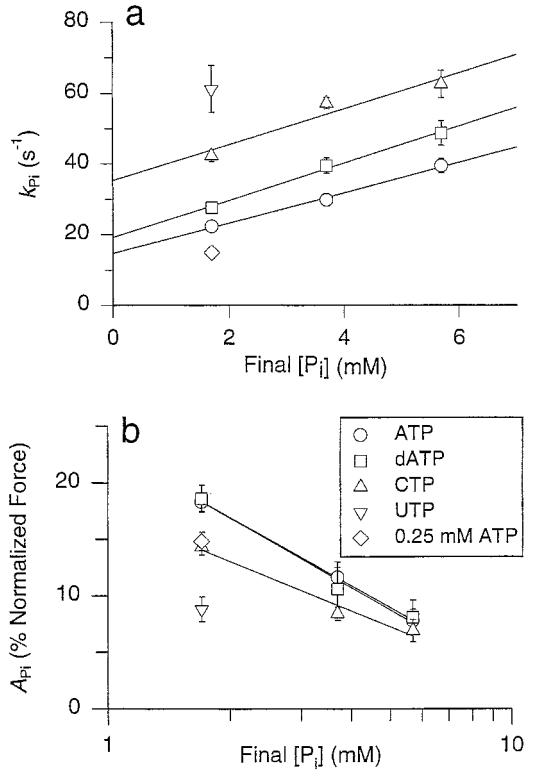

FIGURE 7 $[P_i]$ dependence of k_{Pi} (*a*) and A_{Pi} (*b*). The number of observations (*n*) ranges between 6 and 28 for each data point (mean ± SE) with most $n < 10$. Symbols are the same as for Fig. 4, and some SE bars are too small to be seen. Lines are linear fits to the data with k_{Pi} versus $[P_i]$ slopes of (*a*) 4.3 (ATP), 5.2 (dATP) and 5.1 (CTP) (s^{-1}/mM P_i) and A_{Pi} versus $[P_i]$ slopes of (*b*) −20.0 (ATP), −20.4 (dATP), and −14.5 (CTP) (%/decade P_i). The *y*-intercept values in *a*, used to estimate k_{+5} (Scheme 1), are presented in the text.

6.6 s^{-1}) than for the other nucleotides, suggesting that k_{+5} may be faster for UTP than for dATP and CTP. Measurements of k_{Pi} with NTPs at higher $[P_i]$ were not made because the P_i transient becomes too small to make accurate measurements of k_{Pi} and A_{Pi}. The parallel shift of the $[P_i]$ versus k_{Pi} relationship (Fig. 7 *a*) and the $[P_i]$ versus A_{Pi} relationship (Fig. 7 *b*) for ATP, dATP, and CTP supports the hypothesis that the P_i affinity of cross-bridges is similar in ATP, dATP, and CTP. The $[P_i]$ versus k_{Pi} relationship further suggests that k_{+5} is not the only rate constant of the chemomechanical pathway to be affected by nucleotide type. If k_{+5} alone varied with dATP, CTP, and UTP, P_{NTP} should increase in the same order as k_{Pi}, i.e., ATP < dATP < CTP < UTP. However, P_{NTP} has the relationship UTP < CTP < ATP = dATP, which implies that at least one other rate in the hydrolysis cycle is affected by these nucleotides and that the number of cross-bridges available to enter force-bearing states may be limited in the order UTP < CTP < dATP ≤ ATP (Regnier et al., 1998a).

The effect of shortening on k_{Pi} in different NTP

Recent experiments measuring k_{Pi} during muscle fiber shortening (with ATP) indicate that the force-generating step is strain dependent (Homsher et al., 1997). To determine if the strain sensitivity of this step is affected by nucleotide type, we compared k_{Pi} during fiber shortening with ATP and dATP in the same fiber. Experiments were restricted to a comparison between ATP and dATP, because the force produced by these two nucleotides is similar and they have a similar binding affinity for myosin, making interpretation of the results less complex than with CTP or UTP. Furthermore, because CTP and UTP reduce A_{Pi}, it is difficult to obtain reliable measurements of k_{Pi} during shortening with these nucleotides. In Fig. 8, a fiber was activated to steady state force (shown at the beginning of the recording), then a quick (<2 ms) release (2% L_o, indicated by *asterisks*) followed by a ramp shortening (at 5% of V_u in Fig. 8) reduced force to a near-steady state level at a constant velocity. This procedure quickly reduced force to a new steady-state level that could be maintained during the constant velocity shortening, as shown by trace a. In trace b, the same procedure as the one for trace a was used, but 250

ms after the beginning of shortening, 1 mM P_i was photogenerated from caged P_i in the fiber lattice. As in isometric P_i transients, the resulting rapid force decline is fit well by a single exponential with a rising slope (Homsher et al., 1997). Fig. 9 *a* shows control and P_i transient recordings in dATP, shortening at 0%, 2.5%, 5%, 10%, and 15% of the $V_{u(ATP)}$ measured for this fiber. As the shortening velocity was increased, the time period from the start of shortening to the point at which the laser was flashed (indicated by *arrows*) was decreased to ensure that the P_i transient occurred at a similar sarcomere spacing (2.3–2.5 μm/sarcomere). In Fig. 9 *b* the control recordings in Fig. 9 *a* were subtracted from their corresponding P_i transient traces, and the resultant record was normalized to preflash force for measurements. The force decrease is both smaller and more rapid as fiber shortening velocity is increased. Furthermore, force rebounds to near-steady-state values at higher shortening velocities. Possible reasons for this latter phenomenon are discussed below. The results comparing dATP and ATP are summarized in Fig. 10. At each velocity k_{Pi} is proportionally faster in dATP (compared to ATP), resulting in a parallel shift of the k_{Pi} versus shortening velocity relationship (Fig. 10 *a*). This result suggests that the strain dependence of the force-generating step is not affected by dATP, an interpretation supported by the observation that A_{Pi} is the same for dATP and ATP at each of the shortening velocities used in this study (Fig. 10 *b*).

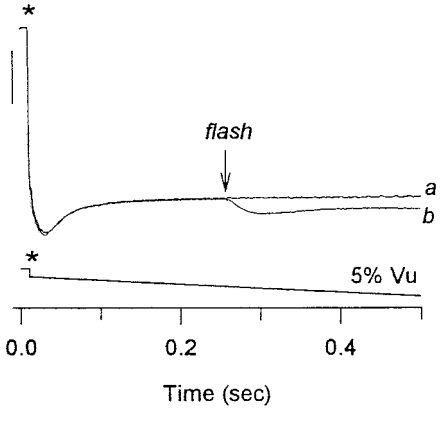

FIGURE 8 Sample force recordings demonstrating the protocol used for measurement of k_{Pi} and A_{Pi} during isovelocity fiber shortening. At the *, a rapid, 2% L_o release was imposed, followed by a ramp shortening at 5% V_u. For recording *a*, force reached a new steady-state level within ~100 ms. For recording *b*, the same procedure was followed, with the exception that 1 mM P_i was photogenerated (indicated by *arrow*) after the new steady-state force level was reached.

DISCUSSION

The measurements of mechanical transients presented above indicate that the force-generating process is altered when ATP is replaced with dATP, CTP, or UTP as the substrate for contractions. Several lines of evidence suggest that the forward rate of the force-generating cross-bridge step (step 5 in Scheme 2) increases in the order ATP < dATP < CTP < UTP:

$$\begin{array}{ccccccc} & 1 & & & 5 & 6 & 7 \\ \mathrm{AM^*{+}NTP} & \leftrightarrow & \mathrm{AM^*.NTP} & \mathrm{AM.NDP.P_i} & \leftrightarrow & \mathrm{AM^*.NDP.P_i} \leftrightarrow \mathrm{AM^*.NDP} & \leftrightarrow \mathrm{AM^*} \\ & 2 \uparrow\downarrow & & \uparrow\downarrow 4 & & & \\ & \mathrm{M.NTP} & \leftrightarrow & \mathrm{M.NDP.P_i} & & & \\ & 3 & & & & & \end{array}$$

Scheme 2

(The asterisks designate force-exerting states.) First, dATP and CTP produce a parallel increase in k_{Pi} with increasing P_i (Fig. 7 *a*). Because the P_{NTP} versus $[P_i]$ relationship for these NTPs (Fig. 1 *a*) exhibits a similar affinity of cross-bridges for P_i, it is unlikely that k_{-5} or K_6 is altered by dATP or CTP. Thus the increased k_{Pi} values in dATP and CTP are probably associated with a faster rate for the force-generating isomerization (k_{+5}). The reduced sensitivity of P_{UTP} to $[P_i]$ may stem from a reduction in the fraction of cross-bridges in the AM* · UDP state. This could result from an increase in k_{-5} or k_{+7} or an accumulation of cross-bridges in the AM, AM · UTP, and M · UTP states, secondary to a slowed UTP cleavage rate, resulting in a reduction AM* · UDP cross-bridges (Regnier et al., 1998a). Second, both k_{tr} (Fig. 4 *a*) and k_{Pi} (Fig. 7 *a*) are dependent on step 5 and increase in the order ATP < dATP < CTP. Finally, dATP produces a parallel increase in k_{Pi} (over ATP) with increasing shortening velocites (Fig. 10), indicating that the increase in k_{+5} in dATP has a strain dependency similar to that for ATP. However, the rate of NDP release from cross-bridges (step 7) must also be faster for dATP, CTP, and UTP, because an increase in k_{+5} alone would increase P_{NTP}, and P_{dATP} is the same as P_o, whereas P_{CTP} and P_{UTP} are reduced (Table 1). A lower affinity of dADP

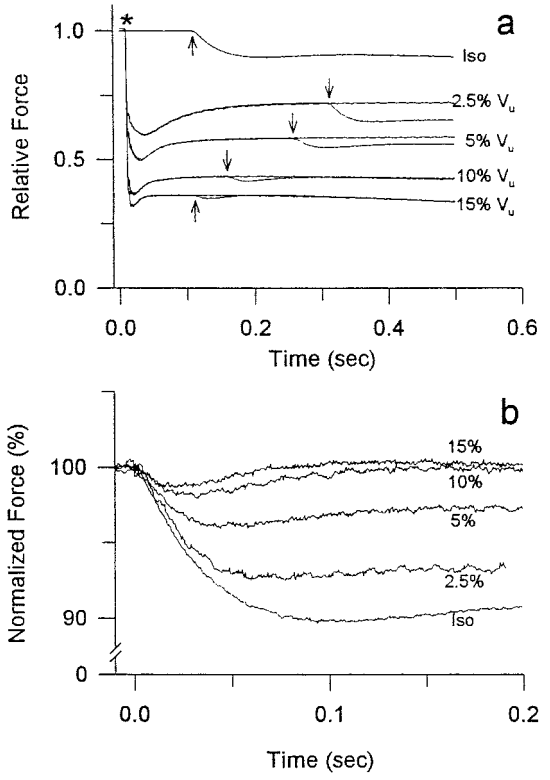

FIGURE 9 Sample force recordings with dATP at several isovelocity shortening speeds, with and without P_i transients. In *a* records are normalized to the prephotolysis force level for the isometric P_i transient. The * indicates when the shortening was begun, using the protocol described in Fig. 8. The ramp shortening rates are indicated next to each set of force traces and are expressed relative to the unloaded shortening velocity, measured for each fiber before P_i transient experiments (Regnier et al., 1998a). Control records (no P_i transient) are shown for each velocity, and the point where 1 mM P_i was photogenerated in matching traces is indicated by arrows. In *b* the control traces were subtracted from traces with P_i transients, and force was normalized to the steady-state level just before the laser flash for measurements of k_{Pi} and A_{Pi}. k_{Pi} and A_{Pi} values for these records are, respectively, 27 s^{-1}, 15%; 43 s^{-1}, 12% (2.5% V_u); 58 s^{-1}, 10% (5% V_u); 94 s^{-1}, 8% (10% V_u); and 138 s^{-1}, 7% (15% V_u).

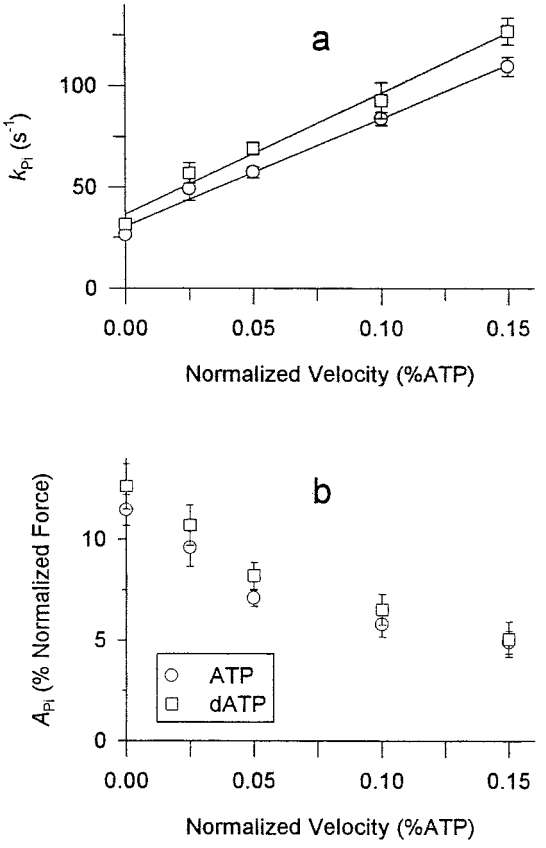

FIGURE 10 Summary of k_{Pi} (*a*) and A_{Pi} (*b*) measurements with isovelocity shortening for ATP and dATP. In *a* linear regression yielded similar slopes of 531 ± 32 (mean ± SE) for ATP and 597 ± 41 s^{-1}/V_u for dATP, indicating that dATP shifted the velocity-k_{Pi} relationship in a parallel manner. In *b* A_{Pi} was not significantly different at any velocity.

for cross-bridges (compared to ADP; M. Geeves, personal communication) supports this idea.

A weaker cross-bridge affinity for CTP and UTP than for ATP suggests that a greater population of rigor (AM*) cross-bridges could exist during contractions at subsaturating concentrations of CTP and UTP (Regnier et al., 1998a). This hypothesis is supported by force measurements during the k_{tr} protocol. The force spike associated with restretching the fiber to its prerelease length is larger and decays at a much slower rate in CTP and UTP than ATP (Fig. 2 *b*), indicating the presence of a population of cross-bridges that is able to rapidly bind to the thin filament and sustain tension rapidly after the restretch. A similar phenomenon occurs at low concentrations of ATP (Fig. 2 *c*), indicating that the larger, longer-lasting force transients during restretch are associated with AM* cross-bridge attachment. The relatively slow dissociation of these cross-bridges obscures the kinetics of force generation at the start of the power stroke, seen at higher nucleotide concentrations (Fig. 2 *c*). Indeed, most of the force redevelopment is obscured by the decay of the force after restretch, save for the last 5–10% of the force rise. Thus the protocol used to measure k_{tr} for the present experiments precludes more precise information about the force-generating step in UTP. Decreasing the concentration of ATP slows V_u, mimicking the effects of CTP and UTP on V_u, but only to a limited extent. Low concentrations of ATP increase isometric force and slow k_{Pi}, whereas CTP and UTP reduce force and increase k_{Pi}. These results show that slower substrate binding to cross-bridges cannot completely explain the effects of CTP and UTP on the mechanics of contraction. The slow rate of UTP cleavage by myosin, reported in the companion paper (Regnier et al., 1998a), suggests that the M · UTP cross-bridge state will be highly populated during contractions. A slowed cleavage step (step 3, Scheme 2) could explain the lower force and stiffness observed in with UTP. In contrast, CTP binds to AM more slowly than ATP and dATP, suggesting a build-up of cross-bridge states at the end of the power stroke, which contribute to force and stiffness, but reduce V_u.

Cross-bridge kinetic simulations in NTP

To test these conclusions and better understand the differences in the kinetics of force production, we used a model (Scheme 3) that describes both k_{tr} and k_{Pi} well for ATP. This model, described in detail by Regnier et al. (1995), does not factor in the strain dependence of cross-bridge interactions, but it does account for the approximately twofold difference between k_{tr} and k_{Pi} under isometric conditions. Scheme 3 includes a calcium-sensitive cross-bridge transition (K_{4a}) from a weakly bound A-M · ADP · P_i state to a strongly bound AM · ADP · P_i state that precedes the force-generating (k_{+5}) step. Moreover, Scheme 3 allowed us to incorporate measured differences in the affinity of NTPs for myosin and the rates of NTP cleavage by myosin and actomyosin to evaluate how these processes influence k_{tr} and k_{Pi}:

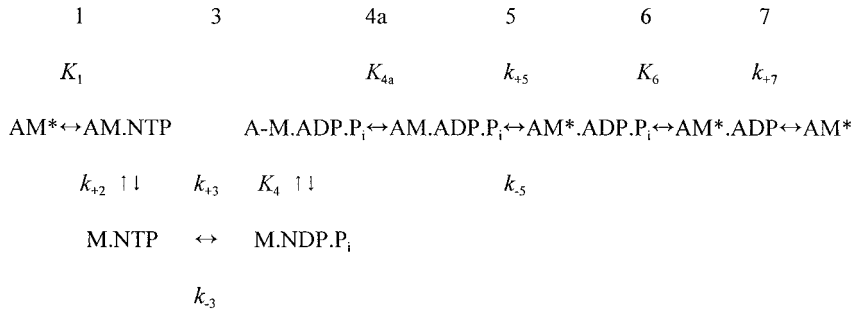

Scheme 3

Simulations of k_{tr} and the P_i transient were made using the rate constants in Table 3. Values for combined steps 1 and 2 ($K_1[NTP]k_{+2}/(K_1[NTP] + 1)$) and for step 3 were taken from the preceding paper (Regnier et al., 1998a), and those for step 5 are from the current paper. The values obtained for steps 1 and 2 in solution suggest that 6 mM ATP dissociates acto-HMM at a rate of $\sim 1 \times 10^3$ s^{-1} ($k_{obs} = K_1[ATP]k_{+2}/(K_1[ATP] + 1)$). Measurements using caged ATP in fibers, however, suggest that K_1k_2 in fibers is as much as an order of magnitude less than in solution, so that cross-bridge dissociation in fibers may occur more slowly than those in solution (Goldman et al., 1984). Part of this reduction may be a consequence of caged ATP binding to the cross-bridges before the photolysis. Variation of $K_1k_{+2}[ATP]/(1 + K_1[ATP])$ from 100 s^{-1} to 1000 s^{-1} had no effect on simulations of k_{tr} or the k_{Pi}, so a value of 500 s^{-1} was arbitrarily chosen for ATP for 6 mM. Thus the value of the rates of cross-bridge dissociation at 6 mM NTP were all $\sim$1/2 of those estimated from solution A-HMM dissociation studies. A weak to strongly bound (but non-force-exerting) cross-bridge isomerization (K_{4a}) regulated by calcium (and preceding the force-generating step) was included, as suggested from Regnier et al. (1995). Inclusion of this step is necessary to account for the almost twofold greater value of k_{Pi}, compared to k_{tr}, measured in these experiments and in previous reports (Regnier et al., 1995; Millar and Homsher, 1990; Walker et al., 1992). We kept K_{4a} (i.e., $K_{4a} = k_{+4a}/k_{-4a} = 30$ $s^{-1}/5$ s^{-1}) constant for modeling of individual NTPs, because the present experiments were all carried out under conditions of maximum Ca^{2+} activation (i.e., pCa 4.5). There is increasing evidence that this step is regulated by thin filament activation processes (McKillop and Geeves, 1993; McKillop et al., 1994; Chase et al., 1994; Regnier et al., 1996, 1998b) and should therefore 1) be independent of nucleotide type and 2) be relatively large at pCa 4.5. Furthermore, the calcium sensitivity of isometric force in psoas fibers is similar for ATP versus CTP (Wahr et al., 1997) and is increased only slightly by dATP (Regnier et al., 1998b). The value for K_6 was taken from earlier work (Dantzig et al., 1992; Millar and Homsher, 1990), adjusted to fit the data in these experiments. For numerical computations of k_{Pi}, rate constants must be assigned to k_{+6} and k_{-6}, and these were taken as 1000 s^{-1} and 6.6×10^4 M^{-1} s^{-1}, respectively (because this step is a rapid equilibrium, the actual values are not important). k_{+6} and k_{-6} were kept the same for simulations in ATP, dATP, and CTP because the force-P_i relationship suggests that the affinity of P_i for cross-bridges is not affected by nucleotide type. For the UTP experiments k_{+6} was reduced by about threefold to bring the force-[P_i]

TABLE 3 Rates (in s^{-1}) used to simulate isometric force, k_{tr}, and k_{Pi} for NTPs in Scheme 3*

NTP	K_1k_{+2}[NTP]/(1 + K_1[NTP])	k_{+3}/k_{-3}	k_{+5}/k_{-5}	k_{+7}
ATP	500	27/18	15/85	3
dATP	500	14/9	22/85	4
CTP	21	42/5	30/85	18
UTP	42	4.3/1.7	50/85	10
Low ATP	21	27/18	15/85	3
Low ATP#	5	27/18	15/85	3

*For all conditions $k_{-1} = 0.01$ s^{-1}, K_4 is rapid, $K_{4a} = 30/5$, $k_{+6} = 1000$ s^{-1}, and $k_{-6} = 6.6 \times 10^4$ M^{-1} s^{-1}.
#K_1k_{+2}[ATP]/(1 + K_1[ATP]) arbitrarily reduced to 5 s^{-1}.

relationship in line. For ATP, k_{+7} was set at 3 s^{-1} to simulate a steady-state ATPase rate of 1–2 s^{-1} in control isometric conditions (Ferenczi and Spencer, 1988). For the other NTPs, k_{+8} was adjusted to offset increases in force (i.e., the sum of AM* · NDP · P_i, AM* · NDP, and AM* states) resulting from higher values of k_{+5} (Table 3). A detailed description of the methods used to simulate k_{Pi} and k_{tr} is presented in Regnier et al. (1995); simulations were analyzed by the same method as for experimental data (see Materials and Methods).

The data in Table 4 show that the rate constants from Table 3 provide simulated values of steady-state force, k_{tr}, k_{Pi}, and A_{Pi}, that are similar to the experimental data (shown in parentheses). Simulations of k_{tr} (Fig. 11) were modeled after a 35-ms period of unloaded shortening (as in the experiments) and show the characteristics of force traces used to measure k_{tr} in fibers (Fig. 2). Simulated force starts from a value near zero for both ATP and dATP, then increases at a similar but slightly faster rate for dATP. In contrast to ATP and dATP, simulations of force redevelopment with CTP, UTP, and 0.25 mM ATP start from much higher levels, mimicking force traces from fibers rather well (compare Figs. 11 and 2, respectively). For CTP, force decays slightly for the first 10–20 ms, then rises at a rate faster than that for ATP and dATP. For UTP and low ATP, force decays slowly for ~100 ms, then rises slowly to the steady-state level. The model predicts that the greater amount of starting force is due to a greater population of rigor cross-bridges (AM* in Scheme 1) at the end of the shortening phase. It must be emphasized, however, that at low [ATP], CTP, and UTP, it is only the reduced values of K_1k_{+2}[NTP]/(1 + K_1[NTP]) used in the simulations that make it possible to fit the relative force and k_{tr} values. If rates greater than 100 s^{-1} are used, relative force and k_{tr} cannot be approximated. This is also evident at low ATP concentrations, in which better approximation to the muscle fiber behavior is obtained when cross-bridge dissociation rates are arbitrarily reduced more than might be expected from the concentrations of ATP alone (i.e., when K_1k_{+2}[ATP]/(1 + K_1 [ATP]) is reduced from 21 s^{-1} to 5 s^{-1}, as shown in Figs. 11 and 12). The quality of the experimental data in CTP and UTP with regard to force and k_{tr} is compromised because CPK does not phosphorylate CDP or UDP fast enough to prevent a build-up of CDP and UDP. This will eventually act to slow the rate of cross-bridge dissociation in the fiber.

TABLE 4 Simulated measurements of release and restretch transients (k_{tr}) and P_i transients (k_{Pi}), using Scheme 3

NTP	Relative force	k_{tr} (s^{-1})	k_{P_i} (s^{-1})	A_{P_i} (%)	NTPase (s^{-1})*
ATP	1	10 (11)	26 (23)	16 (18)	1.3
dATP	0.09 (0.98)	11 (14)	32 (28)	13 (18)	1.7
CTP	0.87 (0.86)	18 (16)	37 (42)	7 (14)	3.6
UTP	0.62 (0.47)	9 (6)	48 (61)	14 (9)	1.6
Low ATP#	1.06 (1.17)	9 (5)	22 (18)	17 (15)	1.2
Low ATP§	1.23 (1.17)	4 (5)	17 (18)	14 (15)	1

*Simulated isometric value.
#For K_1k_{+2}[ATP]/(1 + K_1[ATP]) = 21 s^{-1}.
§For K_1k_{+2}[ATP]/(1 + K_1[ATP]) = 5 s^{-1}.

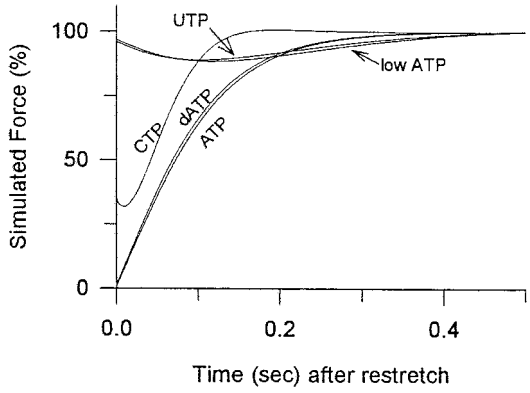

FIGURE 11 Simulations of k_{tr} using Scheme 3. Rate constants used for the simulations are given in Table 3, and simulation details are described in the Discussion.

The behavior of the model suggests that k_{tr} is influenced both by rate constants preceding the force-generating isomerization step and the force-generating isomerization per se. Indeed, the data in Table 2 suggest that the flux through steps 1–5 (Scheme 3) determines k_{tr}. For ATP, the model predicts that after 35 ms of shortening, cross-bridge states are at near-equilibrium values (not shown), with approximately half of the cross-bridges in the precleavage M · ATP state and the other half in the postcleavage, non-force A-M · ADP · P_i and AM · ADP · P_i states. Reducing k_{+3} shifts this equilibrium to the left, and increasing k_{+3} shifts the equilibrium to the right, as for CTP. The changes in k_{+3} used to model dATP and CTP did not greatly influence k_{tr}, which was set mainly by the value of k_{+5}. However, a larger reduction of k_{+3}, either with a concomitant reduction of K_1k_{+2}[NTP]/(1 + K_1[NTP]) (as for UTP) or alone (not shown), eliminates the ability to increase k_{tr} above a basal level of ~3–5 s^{-1} by adjustment of k_{+5}. Large reductions in K_1k_{+2} [NTP]/(1 + K_1[NTP]) alone (as

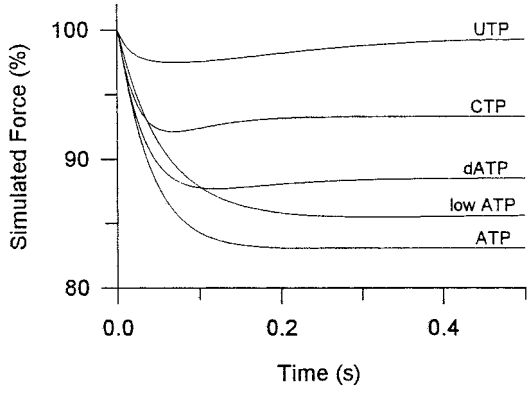

FIGURE 12 Simulations of P_i transients using Scheme 3. Rates used for the simulations are given in Table 3, and simulation details are described in the Discussion.

for low ATP) also prevent an increase in simulated k_{tr} values. This behavior suggests that steps preceding the force-generating isomerization step (step 4a in Scheme 3) influence k_{tr} by limiting the number of cross-bridges available to undergo a force-generating isomerization. A similar conclusion was suggested by experiments comparing k_{tr} at altered levels of Ca^{2+} or P_i in activation solutions or by the addition of butanedione monoxime (BDM) (Regnier et al., 1995).

Decreasing the number of cross-bridges available to enter into force-bearing states, either by substrate limitation (as with low ATP or with UTP) or by lowering the level of activating Ca^{2+}, can account for the slower k_{tr} (relative to k_{Pi}) reported above and in previous studies (Millar and Homsher, 1990; Regnier et al., 1995). As the $[Ca^{2+}]$ of activation solutions is varied in rabbit psoas fibers, the relationship between steady-state force and k_{tr} is curvilinear, such that at low activation levels (i.e., $<50\%$ P_o) k_{tr} is relatively constant, whereas at higher activation levels k_{tr} increases markedly (Brenner, 1988; Metzger and Moss, 1991a; Walker et al., 1992; Chase et al., 1994; Regnier et al., 1996, 1998b). This curvilinear relationship has been explained as Ca^{2+} regulation of the rate of cross-bridge transition from detached or weakly attached states to a more strongly attached state that can then undergo a force-generating isomerization (Millar and Homsher, 1990; Regnier et al., 1995). This regulation may occur via Ca^{2+} regulation of thin filament activation kinetics (Chase et al., 1994; Regnier et al., 1996, 1998b). Alternatively, Ca^{2+} may affect cross-bridges by a more direct mechanism (Brenner, 1988; Metzger and Moss, 1990, 1991a, 1992; Sweeney and Stull, 1990; Walker et al., 1992). In any event, models in which Ca^{2+} regulates a single force-generating step cannot account for the differences between values for k_{tr} and k_{Pi}. Inclusion of a Ca^{2+}-regulated step preceding force generation (step 4a in Scheme 3) produces a Ca^{2+} sensitivity of k_{tr} with little or no Ca^{2+} sensitivity of k_{Pi} (as is seen experimentally), as well as explaining the slower values for k_{tr}. This hypothesis is further supported by measurements of k_{tr} in the presence of calmidazolium (CDZ), a compound that increases the Ca^{2+}-binding affinity of troponin C (Regnier et al., 1996). At submaximum concentrations of Ca^{2+}, CDZ enhances k_{tr} more than steady-state force, suggesting that the kinetics of thin filament activation (preceding force development) can regulate k_{tr}. In the present experiments, the slower cleavage rate of UTP slows k_{tr}, even though the force-generating step (estimated from k_{Pi} measurements) is faster. Reducing the availability of substrate (e.g., at low [ATP]) can reduce k_{tr}, but also reduces k_{Pi}, although to a lesser extent (see below). The increase in k_{tr} and k_{Pi} values with dATP and CTP can be accounted for solely by increasing k_{+5}, with values being estimated from the $[P_i]$ versus k_{Pi} relationship (Fig. 7 *a*). Increasing k_{+5} alone yields similar (simulated) pCa versus force, pCa versus stiffness, and $[P_i]$ versus force curves for ATP, dATP, and CTP (not shown). It also predicts the pCa versus k_{tr} curve reported by Wahr et al. (1997) in CTP. Wahr et al. (1997) concluded that this model could not explain their steady-state force and stiffness data as $[Ca^{2+}]$ was varied, because they primarily altered k_{+4a} in their simulations. This alteration of k_{+4a} does not allow their data to be fitted. However, if k_{+5} is changed as for the case of CTP, the force-pCa data of Wahr et al. (1997) are well fitted by this model.

Changes in k_{Pi} are caused primarily by changes in or subsequent to k_{+5} (Scheme 3). Fig. 12 shows simulation traces of P_i transients. The values obtained for k_{Pi} and A_{Pi}, given in Table 4, basically agree with experimental values (in parentheses for comparison). Further analysis showed that adjusting k_{+5} alone produced simulated P_i transients with k_{Pi} values close to those measured experimentally for dATP, CTP, and UTP, without changing any other rates in Scheme 3. We were unable to simulate a significantly faster k_{Pi} without increasing k_{+5}, but we could decrease k_{tr} with an elevated k_{+5}, suggesting that k_{Pi} more accurately predicted the rate of the force-generating step. Elevation of the rate of NDP release from the cross-bridge (k_{+7}) or the slowing the rate of nucleotide cleavage (k_{+3}) increases the simulated k_{Pi}, but to a lesser degree than increases in k_{+5}.

Surprisingly, P_i transients in 0.25 mM ATP were slower and had a slightly reduced A_{Pi} (Fig. 5 *h* and Table 2). Experimentally these effects on P_i transients do not occur when the [ATP] is reduced from 5 mM to 1 mM, indicating that k_{Pi} is slowed only when the [ATP] is greatly diminished. Likewise, k_{tr} is not slowed until the [ATP] is reduced to $\leq$0.5 mM (Fig. 2 *c* and Regnier et al., 1998b). At concentrations less than or equal to 0.5 mM, k_{tr} rapidly becomes immeasurable, because restretching the fiber results in an immediate return of force to levels greater than or equal to the prerelease force. Model simulations of k_{tr} and k_{Pi} are only slightly slower when $K_1k_{+2}[NTP]/(1 + K_1[NTP])$ is reduced from 500 to 21 s^{-1} (Table 4), but further reduction to 5 s^{-1} yields values of k_{tr}, k_{Pi}, and A_{Pi} that are in good agreement with the experimental data. Examination of the time course of the cross-bridge intermediates after an increase in $[P_i]$ when $K_1k_{+2}[NTP]/(1 + K_1[NTP]) = 5$ s^{-1} show that the before the P_i jump, the AM* state is heavily populated. Its relatively slow decay subsequent to the reduction in cross-bridge flux into the AM* state caused by the P_i jump produces (after the reduction in the AM* · ADP + AM* · ADP · P_i) the slowed decline in force.

Increasing k_{+5} or greatly reducing the rate of NTP cleavage (k_{+3}) caused a reduction in A_{Pi} for simulations of the P_i transient, in agreement with experimental measurements (Table 4). Analysis of the predicted cross-bridge distribution during steady-state force showed a correlation between A_{Pi} and the fraction of AM*ADP cross-bridges available to bind P_i. Interestingly, these manipulations also produced the rebound of force after the initial force decline with increased $[P_i]$ (compare Fig. 5, *d* and *f*, with Fig. 12) seen in CTP and UTP. This force rebound also occurs in P_i transients during shortening, increasing (relative to the A_{Pi}) as the velocity of shortening increases (see Fig. 9), and often when the $[P_i]$ of activation solutions is increased (see Fig. 6). A common link between these conditions is an increase

in the number of detached or weakly attached cross-bridges and an increase in k_{+5}. It may be that the establishment of a new steady-state cross-bridge equilibrium is slowed by these factors, or that the reduction of cross-bridge strain slightly alters the force-P_i relationship within the fiber. Further experiments and the use of a strain-dependent model that includes nucleotide binding and cleavage rates are needed to test this hypothesis.

The authors gratefully acknowledge the assistance of Kerianne Prince.

This work was supported by Public Health Service Grant AR 30988 to EH.

REFERENCES

Araujo, A., and J. W. Walker. 1996. Phosphate release and force generation in cardiac myocytes investigated with caged phosphate and caged calcium. *Biophys. J.* 70:2316–2326.

Brenner, B. 1988. Effect of Ca^{2+} on cross-bridge turnover kinetics in skinned single rabbit psoas fibers: implications for regulation of muscle contraction. *Proc. Natl. Acad. Sci. USA.* 85:3265–3269.

Brenner, B., and E. Eisenberg. 1986. Rate of force generation in muscle: correlation with actomyosin ATPase activity in solution. *Proc. Natl. Acad. Sci. USA.* 83:3542–3546.

Chase, P. B., D. A. Martyn, and J. D. Hannon. 1994. Isometric force redevelopment of skinned muscle fibers from rabbit activated with and without Ca^{2+}. *Biophys. J.* 67:1994–2001.

Cooke, R., K. Franks, G. B. Luciani, and E. Pate. 1988. The inhibition of rabbit skeletal muscle contraction by hydrogen ions and phosphate. *J. Physiol. (Lond.).* 395:77–97.

Dantzig, J. A., Y. E. Goldman, N. C. Millar, J. Lacktis, and E. Homsher. 1992. Reversal of the cross-bridge force-generating transition by photogeneration of phosphate in rabbit psoas muscle fibres. *J. Physiol. (Lond.).* 451:247–278.

Ferenczi, M. A., and I. C. Spencer. 1988. The elementary steps of the actomyosin ATPase in muscle fibres studied with caged-ATP. *Adv. Exp. Med. Biol.* 226:181–188.

Goldman, Y. E., M. G. Hibberd, and D. R. Trentham. 1984. Relaxation of rabbit psoas muscle fibres from rigor by photochemical generation of adenosine-5′-triphosphate. *J. Physiol. (Lond.).* 354:577–604.

Homsher, E., J. Lacktis, and M. Regnier. 1997. Strain-dependent modulation of phosphate transients in rabbit skeletal muscle fibers. *Biophys. J.* 72:1767–1779.

Homsher, E., M. Regnier, and S. Tejeda. 1993. The effect of ATP analogues (NTP) on thin filament movement in motility assays and on the phosphate transient in rabbit glycerinated muscle fibers. *Biophys. J.* 64:A250.

Kentish, J. C. 1991. Combined inhibitory actions of acidosis and phosphate on maximum force production in rat skinned cardiac muscle. *Pflugers Arch.* 419:310–318.

Martyn, D. A., and A. M. Gordon. 1992. Force and stiffness in glycerinated rabbit psoas fibers: effects of calcium and elevated phosphate. *J. Gen. Physiol.* 99:795–816.

McKillop, D. F. A., N. S. Fortune, K. W. Ranatunga, and M. A. Geeves. 1994. The influence of 2,3-butane 2-monoxime (BDM) on the interaction between actin and myosin in solution and in skinned muscle fibres. *J. Muscle Res. Cell Motil.* 15:309–318.

McKillop, D. F. A., and M. A. Geeves. 1993. Regulation of the interaction between actin and mosin subfragment 1: evidence for three states of the thin filament. *Biophys. J.* 65:693–701.

Metzger, J. M., and R. L. Moss. 1990. Calcium-sensitive cross-bridge transitions in mammalian fast and slow skeletal muscle fibers. *Science.* 247:1088–1090.

Metzger, J. M., and R. L. Moss. 1991a. Kinetics of a Ca^{2+}-sensitive cross-bridge transition in skeletal muscle fibers: effects due to variations in thin filament activation by extraction of troponin C. *J. Gen. Physiol.* 98:233–248.

Metzger, J. M., and R. L. Moss. 1991b. Phosphate and the kinetics of force generation in skinned skeletal muscle fibers. *Biophys. J.* 59:418a.

Metzger, J. M., and R. L. Moss. 1992. Myosin light chain 2 modulates calcium-sensitive cross-bridge transitions in vertebrate skeletal muscle. *Biophys. J.* 63:460–468.

Millar, N. C., and E. Homsher. 1990. The effect of phosphate and calcium on force generation in glycerinated rabbit skeletal muscle fibers. *J. Biol. Chem.* 265:20234–20240.

Pate, E., K. Franks-Skiba, H. White, and R. Cooke. 1993. The use of differing nucleotides to investigate cross-bridge kinetics. *J. Biol. Chem.* 268:10046–10053.

Regnier, M., P. Bostani, and E. Homsher. 1993. The effect of ATP analogues (NTP) on isometric force and unloaded shortening velocity (V_{max}) in rabbit glycerinated muscle fibers. *Biophys. J.* 64:A250.

Regnier, M., and E. Homsher. 1996. The effect of NTP binding, cleavage rates, and cleavage equilibrium constants on mechanical behavior of the single rabbit skeletal muscle fiber at 10°C. *Biophys. J.* 70:A290.

Regnier, M., D. M. Lee, and E. Homsher. 1998a. ATP analogues as substrates for muscle contraction: muscle mechanics and kinetics of nucleoside triphosphate binding and hydrolysis. *Biophys. J.* 74: 2005–2015.

Regnier, M., D. A. Martyn, and P. B. Chase. 1996. Calmidazolium alters Ca^{2+} regulation of tension redevelopment rate in skinned skeletal muscle. *Biophys. J.* 71:2786–2794.

Regnier, M., D. A. Martyn, and P. B. Chase. 1998b. Calcium regulation of tension redevelopment kinetics with 2-deoxy-ATP or low [ATP] in skinned rabbit psoas fibers. *Biophys. J.* 74:000–000.

Regnier, M., C. Morris, and E. Homsher. 1995. Regulation of the cross-bridge transition from a weakly to strongly bound state in skinned rabbit muscle fibers. *Am. J. Physiol.* 269:C1532–C1539.

Sweeney, H. L., and J. T. Stull. 1990. Alteration of cross-bridge kinetics by myosin light chain phosphorylation in rabbit skeletal muscle: implications for regulation of actin-myosin interaction. *Proc. Natl. Acad. Sci. USA.* 87:414–418.

Wahr, P. A., H. C. Cantor, and J. M. Metzger. 1997. Nucleotide-dependent contractile properties of Ca^{2+}-activated fast and slow skeletal muscle fibers. *Biophys. J.* 72:822–834.

Walker, J. W., Z. Lu, and R. L. Moss. 1992. Effects of Ca^{2+} on the kinetics of phosphate release in skeletal muscle. *J. Biol. Chem.* 267:2459–2466.

White, H., B. Belnap, and W. Jiang. 1993. Kinetics of binding and hydrolysis of a series of nucleoside triphosphates by actomyosin-S1. *J. Biol. Chem.* 268:10039–10045.